

## Critical Role of Magnesium Ions in DNA Polymerase $\beta$ 's Closing and Active Site Assembly

Linjing Yang,<sup>†</sup> Karunesh Arora,<sup>†</sup> William A. Beard,<sup>‡</sup> Samuel H. Wilson,<sup>‡</sup> and Tamar Schlick<sup>\*†</sup>

Contribution from the Department of Chemistry and Courant Institute of Mathematical Sciences, New York University, 251 Mercer Street, New York, New York 10012, and Laboratory of Structural Biology, National Institute of Environmental Health Sciences, National Institutes of Health, P.O. Box 12233, Research Triangle Park, North Carolina 27709-2233

Received February 2, 2004; E-mail: schlick@nyu.edu

**Abstract:** To dissect the effects of the nucleotide-binding and catalytic metal ions on DNA polymerase mechanisms for DNA repair and synthesis, aside from the chemical reaction, we investigate their roles in the conformational transitions between closed and open states and assembly/disassembly of the active site of polymerase  $\beta$ /DNA complexes before and after the chemical reaction of nucleotide incorporation. Using dynamics simulations, we find that *closing* before chemical reaction requires both divalent metal ions in the active site while *opening* after the chemical reaction is triggered by release of the catalytic metal ion. The critical closing is stabilized by the interaction of the incoming nucleotide with conserved catalytic residues (Asp190, Asp192, Asp256) and the two functional magnesium ions; without the catalytic ion, other protein residues (Arg180, Arg183, Gly189) coordinate the incomer's triphosphate group through the nucleotide-binding ion. Because we also note microionic heterogeneity near the active site,  $Mg^{2+}$  and  $Na^+$  ions can diffuse into the active site relatively rapidly, we suggest that the binding of the catalytic ion itself is not a rate-limiting conformational or overall step. However, geometric adjustments associated with functional ions and proper positioning in the active site, including subtle but systematic motions of protein side chains (e.g., Arg258), define slow or rate-limiting conformational steps that may guide fidelity mechanisms. These sequential rearrangements are likely sensitively affected when an incorrect nucleotide approaches the active site. Our suggestion that subtle and slow adjustments of the nucleotide-binding and catalytic magnesium ions help guide polymerase selection for the correct nucleotide extends descriptions of polymerase pathways and underscores the importance of the delicate conformational events both before and after the chemical reaction to polymerase efficiency and fidelity mechanisms.

### 1. Introduction

Magnesium ions play critical roles in many aspects of cellular metabolism. They stabilize structures of proteins, nucleic acids, and cell membranes by binding to the macromolecule's surface<sup>1–3</sup> and promote specific structural or catalytic activities of proteins, enzymes, or ribozymes. They are also key to enzymatic reactions in various ways. They can generate magnesium-substrate scaffolds, to which enzymes bind; they can bind directly to enzymes and alter their structure; and they may direct reactions through specific catalytic roles. DNA polymerases that replicate and repair DNA employ the critical ions in all these tasks.

DNA polymerases fall into seven families: A, B, C, D, X, Y, and RT based on sequence homologies<sup>4–6</sup> and crystal

structure analysis.<sup>7</sup> Corresponding enzyme/DNA complexes with functional metal ions have been crystallized for several representative DNA polymerases: Klenow fragments of *Escherichia coli*<sup>8</sup> (family A), T7 DNA polymerase<sup>9,10</sup> (family A), *Taq* DNA polymerase (Klentaq1)<sup>11–13</sup> (family A), bacteriophage RB69<sup>14</sup> (family B), DNA polymerase  $\beta$ <sup>15–17</sup> (family X), P2 DNA polymerase IV (Dpo4)<sup>18</sup> (family Y), and human immunodeficiency virus-type 1 (HIV-1) reverse transcriptase (RT)<sup>19</sup> (family

- (6) Braithwaite, D. K.; Ito, J. *Nucleic Acids Res.* **1993**, *21*, 787–802.
- (7) Joyce, C. M.; Steitz, T. A. *Annu. Rev. Biochem.* **1994**, *63*, 777–822.
- (8) Polesky, A. H.; Steitz, T. A.; Grindley, N. D.; Joyce, C. M. *J. Biol. Chem.* **1990**, *265*, 14579–14591.
- (9) Doublie, S.; Ellenberger, T. *Curr. Opin. Struct. Biol.* **1998**, *8*, 704–712.
- (10) Doublie, S.; Tabor, S.; Long, A. M.; Richardson, C. C.; Ellenberger, T. *Nature* **1998**, *391*, 251–258.
- (11) Li, Y.; Korolev, S.; Waksman, G. *EMBO J.* **1998**, *17*, 7514–7525.
- (12) Li, Y.; Mitaxov, V.; Waksman, G. *Proc. Natl. Acad. Sci. U.S.A.* **1999**, *96*, 9491–9496.
- (13) Li, Y.; Waksman, G. *Protein Sci.* **2001**, *10*, 1225–1233.
- (14) Wang, J.; Satter, A. K. M. A.; Wang, C. C.; Karam, J. D.; Konigsberg, W. H.; Steitz, T. A. *Cell* **1997**, *89*, 1087–1099.
- (15) Sawaya, M. R.; Pelletier, H.; Kumar, A.; Wilson, S. H.; Kraut, J. *Science* **1994**, *264*, 1930–1935.
- (16) Sawaya, M. R.; Prasad, R.; Wilson, S. H.; Kraut, J.; Pelletier, H. *Biochemistry* **1997**, *36*, 11205–11215.
- (17) Pelletier, H.; Sawaya, M. R.; Kumar, A.; Wilson, S. H.; Kraut, J. *Science* **1994**, *264*, 1891–1903.
- (18) Ling, H.; Boudsocq, F.; Woodgate, R.; Yang, W. *Cell* **2001**, *107*, 91–102.

\* Corresponding author.

<sup>†</sup> New York University.

<sup>‡</sup> National Institute of Environmental Health Sciences.

- (1) Cowan, J. A. *The Biological chemistry of magnesium*; VCH publishers, Inc.: New York, 1995.
- (2) Cowan, J. A. *Inorganic biochemistry. An introduction*; VCH publishers, Inc.: New York, 1993.
- (3) Burgess, J. *Ions in solution: basic principles of chemical interaction*; Ellis Horwood, Ltd.: New York, 1988.
- (4) Delarue, M.; Poch, O.; Tordo, N.; Moras, D.; Argos, P. *Protein Eng.* **1990**, *3*, 461–467.
- (5) Ito, J.; Braithwaite, D. K. *Nucleic Acids Res.* **1991**, *19*, 4045–4057.

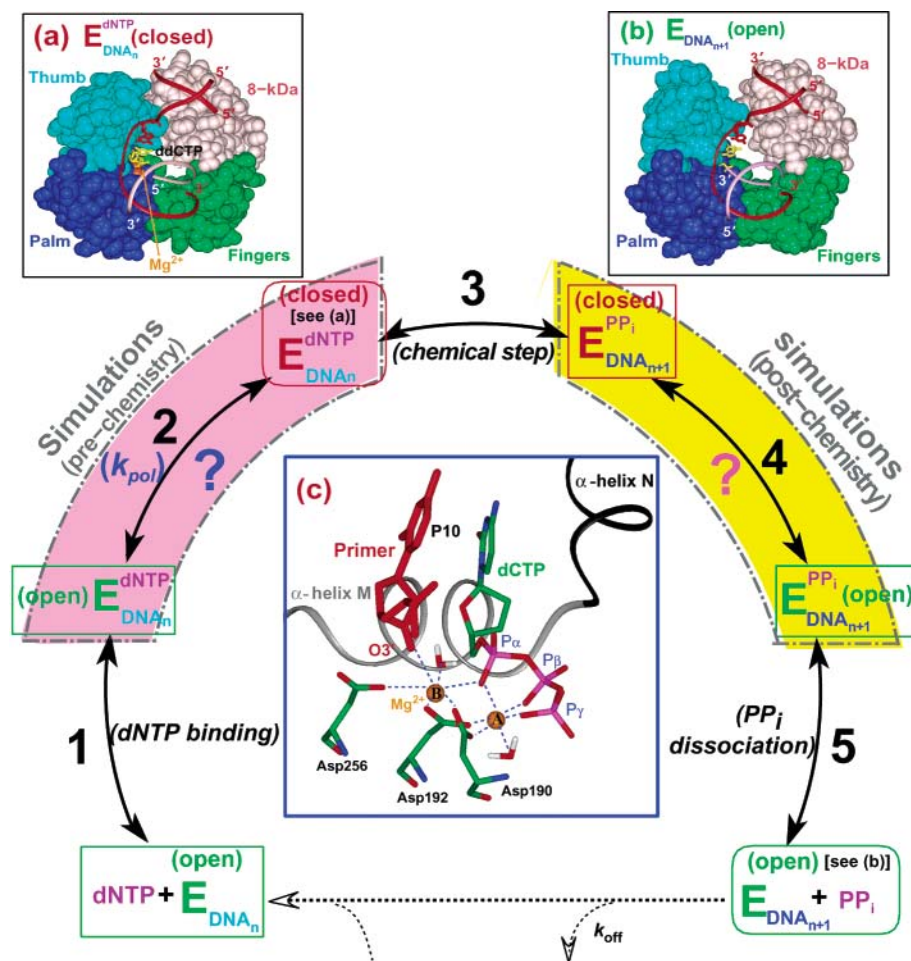


**Figure 1.** A general pathway for nucleotide incorporation by DNA polymerases is thought to apply to DNA polymerases with distinct open and closed states; crystallographic (a) closed and (b) open conformations of polymerase  $\beta$ /DNA complex along the pathway are used for illustration. E, dNTP, and PP<sub>i</sub> refer to DNA polymerase, 2'-deoxyribonucleoside 5'-triphosphate, and pyrophosphate, respectively. DNA<sub>n</sub> and DNA<sub>n+1</sub> represent the DNA before and after the nucleotide incorporation to the DNA primer 3'-terminus. Red and green distinguish the crystal closed and open states of polymerase/DNA complexes, respectively. The highlighted pink and yellow arcs represent polymerase  $\beta$ 's conformational closing (before the chemical reaction) and opening (after the chemical reaction) motions, respectively, which we investigate here. See text for detailed description of the polymerase catalytic cycle. (c) Active-site coordination of the nucleotide-binding (label A) and catalytic (label B) Mg<sup>2+</sup> in the closed ternary pol  $\beta$ /DNA/dCTP complex. In part c, the nucleotide-binding Mg<sup>2+</sup> coordinates the  $\alpha$ -,  $\beta$ -, and  $\gamma$ -phosphate oxygens from dCTP, Asp190, Asp192, and one water molecule; and, the catalytic Mg<sup>2+</sup> coordinates the  $\alpha$ -phosphate oxygen from dCTP, primer P10:O3', Asp190, Asp192, Asp256, and one water molecule.

RT). Although sequence similarity across families of DNA polymerases is low, common is a two-metal-ion (usually Mg<sup>2+</sup>) coordination with a few conserved acidic residues (e.g., two highly conserved carboxylate-containing residues such as aspartates and possibly an additional residue like aspartate or glutamate) in the enzyme active site.<sup>4,14</sup> This conservation of the metal-binding site in highly divergent DNA polymerases underscores the importance of the metal ions in assisting nucleotide polymerization.

Experimental kinetic analyses for several high or medium-fidelity DNA polymerases (*E. coli* DNA polymerase I Klenow fragment,<sup>20,21</sup> T7 DNA polymerase,<sup>22</sup> HIV-1 reverse transcriptase,<sup>23</sup> T4 DNA polymerase,<sup>24</sup> and DNA polymerase  $\beta$ <sup>25–27</sup>)

have suggested rate-limiting conformational changes in polymerases both before and after the chemical reaction of nucleotide incorporation in DNA synthesis. Combined with the available crystallographic open and closed structures of several polymerases complexed with primer/template duplex DNA and/or incoming nucleotide,<sup>9–17,19</sup> a general pathway for nucleotide insertion by DNA polymerases has been delineated, as sketched in Figure 1. Namely, a DNA polymerase binds DNA to form a binary complex in an open state, which further binds a correct 2'-deoxyribonucleoside 5'-triphosphate (dNTP) to form an open ternary complex (step 1). This open complex undergoes a conformational transition to generate a closed ternary complex (step 2), in which the chemical reaction of incorporating dNTP to the primer 3'-terminus (step 3) occurs. Following the chemical reaction, the product complex undergoes a second conformational change from a closed to an open state (step 4) prior to

(19) Huang, H.; Chopra, R.; Verdine, G. L.; Harrison, S. C. *Science* **1998**, *282*, 1669–1675.

(20) Kuchta, R. D.; Benkovic, P.; Benkovic, S. J. *Biochemistry* **1988**, *27*, 6716–6725.

(21) Dahlberg, M. E.; Benkovic, S. J. *Biochemistry* **1991**, *30*, 4835–4843.

(22) Patel, S. S.; Wong, I.; Johnson, K. A. *Biochemistry* **1991**, *30*, 511–525.

(23) Kati, W. M.; Johnson, K. A.; Jerva, L. F.; Anderson, K. S. *J. Biol. Chem.* **1992**, *267*, 25988–25997.

(24) Frey, M. W.; Sowers, L. C.; Millar, D. P.; Benkovic, S. J. *Biochemistry* **1995**, *34*, 9185–9192.

(25) Werneburg, B. G.; Ahn, J.; Zhong, X.; Hondal, R. J.; Kraynov, V. S.; Tsai, M.-D. *Biochemistry* **1996**, *35*, 7041–7050.

(26) Zhong, X.; Patel, S. S.; Werneburg, B. G.; Tsai, M.-D. *Biochemistry* **1997**, *36*, 11891–11900.

(27) Vande Berg, B. J.; Beard, W. A.; Wilson, S. H. *J. Biol. Chem.* **2001**, *276*, 3408–3416.

release of the product pyrophosphate (PP<sub>i</sub>) (step 5). Such conformational alterations between closed and open states help maintain DNA polymerase fidelity, choosing the correct incoming nucleotide via an “induced-fit” mechanism.<sup>16,28–31</sup>

Many DNA polymerases are known to incorporate nucleotides to the DNA primer strand through a “two-metal-ion” mechanism<sup>32</sup> in a closed state. The nucleotide-binding ion coordinates the  $\alpha$ -,  $\beta$ -, and  $\gamma$ -phosphate oxygens of the incoming dNTP; the catalytic ion coordinates both the  $\alpha$ -phosphate of dNTP and the 3'-O of the primer strand (Figure 1c). Coordination of the catalytic ion to the primer 3'-O facilitates the chemical reaction, in-line nucleophilic attack of 3'-OH on dNTP's P <sub>$\alpha$</sub> . The position and geometry of P <sub>$\alpha$</sub>  are stabilized through interactions of the two nonbridging oxygens on P <sub>$\alpha$</sub>  (Pro-S<sub>p</sub> and Pro-R<sub>p</sub>) with protein residues and two functional metal ions in the active site.<sup>33</sup>

In some medium- or low-fidelity DNA polymerases such as pol  $\beta$ <sup>16</sup> and Dpo4,<sup>18</sup> the P <sub>$\alpha$</sub> 's Pro-S<sub>p</sub> oxygen does not contact any protein residues, but the Pro-R<sub>p</sub> oxygen coordinates one or both of the functional metal ions.<sup>33</sup> The nucleotide-binding metal ion assists the departure of the product pyrophosphate from the active site, and both ions help stabilize the structure of the expected pentacovalent transition state in the chemical reaction of nucleotide addition. This “two-metal-ion” functional mechanism has thus been implicated with assembling the catalytic groups, neutralizing the negative charges of the environment, stabilizing the active site structure, and catalyzing the nucleotide insertion. The roles of the metal ions in the catalytic chemical reaction have been studied by many experimentalists and theoreticians, including the leading groups of Warshel, Truhlar, Goodman, Karplus, and Gao.<sup>34–36</sup> In particular, the Warshel and Goodman groups recently reported pioneering work to delineate pathways in the chemical reaction of nucleotide insertion for T7 DNA polymerase and DNA polymerase  $\beta$ .<sup>34,37</sup> However, the complementary aspect regarding the distinctive role of each functional metal ion in regulating polymerase transitions between closed and open states (aside from the chemical reaction) and in polymerase fidelity remains uncertain and is the subject of this work. Here we separately examine by dynamics simulations the effects of the nucleotide-binding Mg<sup>2+</sup> and the catalytic Mg<sup>2+</sup> on DNA polymerase  $\beta$  (pol  $\beta$ ) conformational changes between closed and open states both before and after the chemical reaction of nucleotide incorporation to gain insights into polymerase efficiency and fidelity.

DNA polymerase  $\beta$  is an attractive model to study polymerase mechanisms in DNA synthesis due to its small size and a large amount of available experimental kinetic data<sup>25–27,38–40</sup> and

X-ray crystallographic structures at high-resolution.<sup>15–17,41</sup> Pol  $\beta$ 's 335 residues define two domains: an N-terminal 8-kDa which exhibits deoxyribosephosphate lyase activity and a C-terminal 31-kDa which possesses nucleotidyl transfer activity.<sup>42</sup> Most DNA polymerases share a handlike overall architecture.<sup>43</sup> Pol  $\beta$ 's 31-kDa domain resembles a left-hand with “thumb”, “palm”, and “fingers” subdomains. In the crystallographic *closed ternary* complex of pol  $\beta$ /DNA/ddCTP,<sup>16</sup> the nucleotide-binding and catalytic Mg<sup>2+</sup> ions are both coordinated to the active site groups, as shown in Figure 1c. Both ions are missing in the crystallographic *open gapped* and *nicked* pol  $\beta$ /DNA complexes.<sup>16</sup> The polymerase catalytic cycle proceeds from an “open” gapped DNA binary complex to a “closed” ternary complex to an “open” nicked DNA binary complex. The “open” gapped complex before the chemical reaction and the “open” nicked complex after the chemical reaction are nearly superimposable except for some local side chains. For instance, Asp192 rotates toward Arg258 to form a salt bridge in the open gapped complex, while it does not in the open nicked complex.<sup>16</sup> These crystallographic open and closed pol  $\beta$ /DNA complexes provide the structural basis for studying the effect of the functional Mg<sup>2+</sup> ions on pol  $\beta$ 's conformational closing and opening and thus pol  $\beta$  fidelity.

We separately examine behaviors of pol  $\beta$ /DNA complexes with one, two, or no magnesium ions in the active site before, as well as after, the nucleotide chemical incorporation using dynamics simulations over 10.5 ns. Certainly, our dynamics simulations performed even with the state-of-the-art CHARMM force field suffer from inherent limitations, such as force-field uncertainties, solvent approximations, limited sampling, and finite size effects. In particular, there are shortcomings of the current treatment of divalent ions: the short-range interactions involving divalent ions have a common artifact in force field which uses a sum of Lennard–Jones and electrostatic interactions to reproduce the experimental free energy of ion solvation.<sup>44–46</sup> Such interactions between ions and ligands may be understabilized and, thus, may result systematically in shorter ligand/ion distances compared to those in the crystallographic structures. Moreover, the short-range effects may affect fine details of the active site geometry and dynamics. Nonetheless, because our studies focus more on macroscopic long-range effects of the divalent ions (e.g., effects of active-site magnesium ions on thumb motions in pol  $\beta$ ), it is reasonable to assume that the short-range interactions will have a smaller influence on our main interpretations.

Our results indicate that pol  $\beta$ 's closing before the chemical reaction is hampered when one or both ions are not present and, similarly, that opening after the chemical reaction is slowed when both ions are present. Thus, pol  $\beta$ 's closing transition is stabilized by binding the magnesium-ion bound dNTP (“induced-fit” hypothesis) plus the catalytic Mg<sup>2+</sup>. The concomitant interactions, between the dNTP's triphosphate group and protein

- (28) Koshland, D. E. *Angew. Chem., Int. Ed. Engl.* **1994**, *33*, 2375–2378.  
(29) Wong, I.; Patel, S. S.; Johnson, K. A. *Biochemistry* **1991**, *30*, 526–537.  
(30) Echols, H.; Goodman, M. F. *Annu. Rev. Biochem.* **1991**, *60*, 477–511.  
(31) Beard, W. A.; Wilson, S. H. *Chem. Biol.* **1998**, *5*, R7–R13.  
(32) Steitz, T. A. *Curr. Opin. Struct. Biol.* **1993**, *3*, 31–38.  
(33) Beard, W. A.; Wilson, S. H. *Structure* **2003**, *11*, 489–496.  
(34) Florián, J.; Goodman, M. F.; Warshel, A. *J. Am. Chem. Soc.* **2003**, *125*, 8163–8177.  
(35) García-Viloca, M.; Gao, J.; Karplus, M.; Truhlar, D. G. *Science* **2003**, *303*, 186–194.  
(36) Warshel, A. *Computer Modeling of Chemical Reactions in Enzymes and Solutions*. John Wiley & Sons: New York, 1991.  
(37) Florián, J.; Goodman, M. F.; Warshel, A. *Biopolymers* **2003**, *68*, 286–299.  
(38) Ahn, J.; Werneburg, B. G.; Tsai, M.-D. *Biochemistry* **1997**, *36*, 1100–1107.  
(39) Ahn, J.; Kraynov, V. S.; Zhong, X.; Werneburg, B. G.; Tsai, M.-D. *Biochem. J.* **1998**, *331*, 79–87.  
(40) Shah, A. M.; Li, S.-X.; Anderson, K. S.; Sweasy, J. B. *J. Biol. Chem.* **2001**, *276*, 10824–10831.

- (41) Krahn, J. M.; Beard, W. A.; Miller, H.; Grollman, A. P.; Wilson, S. H. *Structure* **2003**, *11*, 121–127.  
(42) Beard, W. A.; Wilson, S. H. *Mutat. Res.* **2000**, *460*, 231–244.  
(43) Ollis, D. L.; Brick, P.; Hamlin, R.; Xuong, N. G.; Steitz, T. A. *Nature* **1985**, *313*, 762–766.  
(44) Brooks, B. R.; Brucoleri, R. E.; Olafson, B. D.; States, D. J.; Swaminathan, S.; Karplus, M. *J. Comput. Chem.* **1983**, *4*, 187–217.  
(45) Stote, R. H.; Karplus, M. *Proteins* **1995**, *23*, 12–31.  
(46) MacKerell, J. A. D. *J. Phys. Chem. B* **1997**, *101*, 646–650.



residues Asp190, Asp192, Asp256, and Asp276, as well as with both  $Mg^{2+}$  ions, help stabilize the pol  $\beta$  in the closed conformation required for the chemical reaction. When only the nucleotide-binding ion is present, the dNTP's triphosphate group and protein residues Ser180, Arg183, and Gly189 can pull the dNTP away from the primer 3'-terminus, triggering an opening rather than closing as needed.

Furthermore, our observed microheterogeneity of ions at the active site after the chemical reaction, based on diffusion of a solution  $Na^+$  counterion into the active site within 1 ns from 30 Å away and its coordination with Asp190, Asp192, and/or Asp256, and migration of a solution  $Mg^{2+}$  (along with its coordinated six water molecules) into the active site within 3 ns from 20 Å away, suggest that the binding of the catalytic metal ion to the polymerase active site is relatively fast and not rate-limiting. However, associated slow motions of side chains in the active site point to crucial geometric adjustments of catalytic groups including key protein residues, the incoming nucleotide, primer 3'-OH terminus, and both metal ions before the chemical reaction, after polymerase closing, as supervisors of the fidelity process.

Such slow local geometric adjustments will be crucially affected by binding an incorrect nucleotide, triggering dissociation. Our work thus extends current views of polymerase mechanisms by suggesting how the divalent ions regulate not only the chemical reaction itself but also its occurrence (via systematic preparation of the active site before the chemical reaction and its disassembly after the chemical reaction) through slow, subtle conformational changes that may guide fidelity mechanisms.

## 2. Methods

**2.1. Systems Setup.** Eight pol  $\beta$ /DNA complexes were constructed: four models before and four models after the chemical reaction of nucleotide incorporation, each case representing an intermediate structure between closed and open states, and each quadruplet involving a nucleotide-binding  $Mg^{2+}$ , catalytic  $Mg^{2+}$ , both  $Mg^{2+}$  ions, or no  $Mg^{2+}$ . The four initial models after the chemical reaction were constructed on the basis of a postchemistry intermediate, which was built as an average of the PDB/RCSB<sup>47</sup> coordinate entries IBPY (closed, ternary complex) and IBPZ (open, binary nicked complex); see details in our previous studies.<sup>48,49</sup> The four initial models before the chemical reaction were constructed on the basis of a prechemistry intermediate, which was built as an average of PDB/RCSB<sup>47</sup> coordinate entries IBPX (open, binary gapped complex) and IBPY.<sup>16</sup> The missing protein residues 1–4 in the open gapped binary complex and residues 1–9 in the ternary closed complex were added using the InsightII package, version 2000. An OH group was added to the primer P10/dC:C3' and the ddCTP:C3' in the closed structure, but the dCTP has not been connected to the primer strand for construction of the prechemistry intermediate. All hydrogen atoms were added by CHARMM's HBUILD routine.<sup>44,50,51</sup> Both of the constructed intermediate models resemble well a crystallographic structure of an intermediate pol  $\beta$ /DNA complex with a mismatched CA pair after the nucleotide chemical incorporation (Krahn,

Beard, and Wilson, submitted).<sup>48</sup> Moreover, the prechemistry intermediate likely lies on pol  $\beta$ 's closing pathway as recently delineated by a stochastic pathway approach.<sup>52</sup>

Based on the postchemistry intermediate, the PP<sub>i</sub>/ $Mg^{2+}$  association was placed in the active site with the  $Mg^{2+}$  coordinating two phosphate oxygens of PP<sub>i</sub>, Asp190, and Asp192, and/or the catalytic  $Mg^{2+}$  was placed to coordinate Asp190, Asp192, Asp256, and the primer P10:O3' in the corresponding pol  $\beta$ /DNA complexes with one or both  $Mg^{2+}$  ions after the chemical reaction. On the basis of the prechemistry intermediate, the dCTP/ $Mg^{2+}$  association and/or the catalytic  $Mg^{2+}$  were positioned in the active site, similar to those in the crystal closed ternary complex,<sup>16</sup> in the corresponding pol  $\beta$ /DNA systems with one or both  $Mg^{2+}$  ions before the chemical reaction. The postchemistry complexes were solvated in a periodic domain of face-centered cube while the prechemistry complexes in a periodic cube domain with smallest image distance of 16 Å. All systems were neutralized by  $Na^+$  and  $Cl^-$  counterions at an ionic strength of 150 mM, as in our previous studies.<sup>48,49</sup> Thus, this modeling produces four solvated intermediate models of pol  $\beta$ /DNA *after chemical reaction* with the following: the PP<sub>i</sub>/ $Mg^{2+}$  complex (termed as post-nuc, 41 986 atoms), the catalytic  $Mg^{2+}$  (termed as post-cat, 41 977 atoms), both  $Mg^{2+}$  (termed as post-both, 41 987 atoms), or none of  $Mg^{2+}$  (termed as post-none, 41 973 atoms). Similarly, the modeling produces four solvated intermediate models of pol  $\beta$ /DNA *before chemical reaction* with the following: the dCTP/ $Mg^{2+}$  complex (termed as pre-nuc, 39 992 atoms), the catalytic  $Mg^{2+}$  (termed as pre-cat, 39 992 atoms), both  $Mg^{2+}$  (termed as pre-both, 39 995 atoms), or none of  $Mg^{2+}$  (termed as pre-none, 39 953 atoms). The thumb subdomain of pol  $\beta$  in all these intermediate models is partially open (i.e., the rmsd of  $\alpha$ -helix N in the intermediate model is about 4 and 3 Å relative to the crystal open and closed structures, respectively, while the  $\alpha$ -helix N rmsd between the crystal open and closed structures is about 7 Å). All these simulations involving functional ions from an intermediate structure allow direct comparison to our prior simulations.<sup>48,49,53</sup>

**2.2. Minimization, Equilibration, and Dynamics Protocol.** We use the all-atom version 26a2 CHARMM force field<sup>44,51</sup> (Chemistry Department, Harvard University, Cambridge, MA) to perform energy minimizations, equilibrations, and dynamics simulations for all systems. First, each system was minimized for 10 000 steps of the steepest descent (SD) method followed by 20 000 steps of adapted basis Newton–Raphson (ABNR)<sup>44,54</sup> while fixing positions of all heavy atoms of pol  $\beta$ /DNA; second, each system was further minimized by SD and ABNR without any restraints until the energy gradient was less than  $10^{-6}$  kcal/mol Å. Then, each system was equilibrated for 30 ps at room temperature by using the stochastic LN integrator<sup>55–58</sup> before the 10.5 ns dynamics production began.

The multiple time step LN integrator<sup>55–57</sup> is efficient for propagating large biomolecular dynamics according to the Langevin equation. The LN protocol of  $\Delta\tau/\Delta t_m/\Delta t = 1/2/150$  fs has been demonstrated to be stable and reliable in terms of thermodynamic, structural, and dynamic properties compared to single-time step Langevin as well as Newtonian (Velocity Verlet) propagators<sup>48</sup> and has been applied to several simulations of pol  $\beta$ /DNA complexes in our previous works.<sup>48,49</sup> In this multiple time step LN protocol, the inner time step  $\Delta\tau$  is for calculating the bond, bond-angle, and dihedral energy terms; the medium time step  $\Delta t_m$  is used for updating the nonbonded interactions within

- (47) Berman, H. M.; Westbrook, J.; Feng, Z.; Gilliland, G.; Bhat, T. N.; Weissig, H.; Shindyalov, I. N.; Bourne, P. E. *Nucleic Acids Res.* **2000**, *28*, 235–242.  
 (48) Yang, L.; Beard, W. A.; Wilson, S. H.; Broyde, S.; Schlick, T. *J. Mol. Biol.* **2002**, *317*, 651–671.  
 (49) Yang, L.; Beard, W. A.; Wilson, S. H.; Roux, B.; Broyde, S.; Schlick, T. *J. Mol. Biol.* **2002**, *321*, 459–478.  
 (50) Brünger, A. T.; Karplus, M. *Proteins: Struct., Funct., Genet.* **1988**, *4*, 148–156.  
 (51) MacKerell, A. D., Jr.; Banavali, N. K. *J. Comput. Chem.* **2000**, *21*, 105–120.

- (52) Arora, K.; Schlick, T. The complete closing conformational transition pathway of polymerase  $\beta$  simulated using stochastic difference equation algorithm. In preparation.  
 (53) Yang, L.; Beard, W. A.; Wilson, S. H.; Broyde, S.; Schlick, T. *Biophys. J.* **2004**, *86*, 1–17.  
 (54) Schlick, T. In *Reviews in Computational Chemistry*; Lipkowitz, K. B.; Boyd, D. B., Eds.; VCH Publishers: New York, 1992; Vol. III, pp 1–71.  
 (55) Schlick, T.; Barth, E.; Mandziuk, M. *Annu. Rev. Biophys. Biomol. Struct.* **1997**, *26*, 181–222.  
 (56) Barth, E.; Schlick, T. *J. Chem. Phys.* **1998**, *109*, 1617–1632.  
 (57) Barth, E.; Schlick, T. *J. Chem. Phys.* **1998**, *109*, 1633–1642.  
 (58) Schlick, T. *Structure* **2001**, *9*, R45–R53.

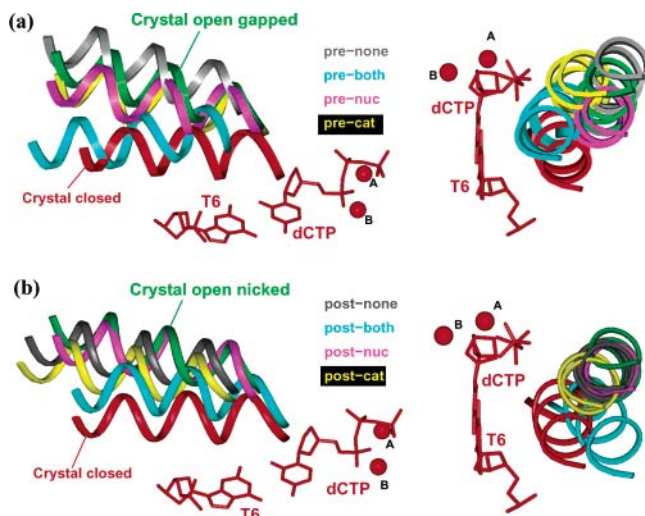


**Figure 2.** Comparison of  $\alpha$ -helix N positions in the simulated systems both (a) before and (b) after the chemical reaction of nucleotide incorporation with respect to those in the crystal open and closed structures. All systems are superimposed according to the palm C $\alpha$  atoms. The colored ribbons red, green, gray, blue, pink, and yellow indicate the closed crystal, the open crystal structure, and the simulated pol  $\beta$ /DNA complexes with no Mg<sup>2+</sup>, both Mg<sup>2+</sup>, the nucleotide-binding Mg<sup>2+</sup>, or the catalytic Mg<sup>2+</sup>, respectively. The rectangular (upper) and oval (lower) ribbons indicate the simulated systems before and after the chemical reaction, respectively. The positions of  $\alpha$ -helix N in all systems are shown from two points of view.

a spherical distance (here 7 Å and associated with healing and buffer lengths of 4 Å each); and the outer time step is for updating the remaining nonbonded interactions up to the global nonbonded interaction cutoff distance (14 Å here). This updating utilizes a heuristic procedure if any atom moves more than 1 Å. Electrostatic and van der Waals interactions are smoothed to zero at 12 Å with a shift function and a switch function, respectively. The Langevin collision parameter of  $\gamma = 10 \text{ ps}^{-1}$  is used to couple the system to a 300 °C heat bath. The SHAKE algorithm was employed in all runs to constrain the bonds involving hydrogens. The computational speedup for our large pol  $\beta$ /DNA systems with LN are around 5 with respect to the single time step of 1 fs with Langevin.<sup>48</sup>

### 3. Results

**3.1. Closing Is Opposed unless Both Ions Are Present, and Opening Is Encouraged if Either Ion is Absent.** The  $\alpha$ -helix N in the thumb subdomain rotates significantly during pol  $\beta$ 's conformational transitions between open and closed states<sup>16</sup> and is thus a good measure of this large-scale motion. Figure 2 shows the positions of  $\alpha$ -helix N in all systems after 10.5 ns simulation both before and after the chemical reaction relative to those in the crystal open and closed structures, and Figure 3 quantifies these closing/opening trends via  $\alpha$ -helix N's rmsd values. (The rmsd values for the prechemistry system with both ions are modified due to the  $\alpha$ -helix N's parallel movement with respect to those in the crystal closed and open structures. See Supporting Information for detailed calculations.) Opening, rather than closing, motions are clearly observed when one or both ions are missing before the chemical reaction; both ions, however, are associated with a closing trend as required (see Figure 2a). Since the  $\alpha$ -helix N in the simulated system with both ions is not superimposable to that in the crystal closed structure, full closing likely requires a longer time. After the chemical reaction, opening as expected is pronounced when one or no ions are present but is clearly less favored in the presence of both ions.

We also calculate the interactions between the active-site base pair (or only the template base T6 when the dCTP/Mg<sup>2+</sup> is not present) and  $\alpha$ -helix N in all trajectories as a function of time, as shown in Figure S1 (Supporting Information). These interactions become stronger when both ions are present, both before and after the chemical reaction. The interaction variations are consistent with the  $\alpha$ -helix N motions in the corresponding systems (Figure 2).

In sum, these closing/opening trends suggest that the two Mg<sup>2+</sup> ions together in the active site may help stabilize pol  $\beta$  in a closed state and thereby not only help organize the reaction-competent state but also direct its formation.

### 3.2. Sequence of Events in Pol $\beta$ 's Closing and Opening Both before and after the Chemical Reaction.

The sequence of events in pol  $\beta$ 's closing and opening involving the local subtle motions for all trajectories can be analyzed from Figures 4 and 5. In the prechemistry simulation with both Mg<sup>2+</sup> ions (pre-both), pol  $\beta$  moves slightly toward a closed state. Since our initial models for all systems are constructed in an intermediate structure between closed and open states, the thumb is in a partially closed state at the start of this simulation (the  $\alpha$ -helix N rmsd being  $\sim 4$  Å relative to the crystal closed and  $\sim 6$  Å relative to the crystal open), and Asp192 rotates to coordinate both Mg<sup>2+</sup> ions after energy minimization (before the productive dynamics runs). The Phe272 ring flips toward Asp192 early in the simulation (monitored by the time evolution of dihedral angles  $\chi_1$  and  $\chi_2$  described in the caption of Figure 4), similar to its position in the closed structure, and flips back again incompletely ( $147^\circ < 160^\circ$  for  $\chi_1$ ) later (see Figure 4). The  $\sim 4$  Å distance between Arg258:NH1 and Tyr296:OH throughout the entire pre-both simulation indicates that Arg258 is in a position similar to the crystal closed structure<sup>16</sup> (Figures S2,5). In general, this trajectory with both Mg<sup>2+</sup> ions suggests the following sequence of events in pol  $\beta$ 's closing *before the chemical reaction*: (1) partial thumb closing, (2) rotation of Asp192 to coordinate both ions, (3) flip of Phe272, and (4) full enzyme closing. This sequence of events is approximately consistent with that proposed by the novel pathway methodology applications on pol  $\beta$ /DNA complexes before the chemical reaction.<sup>59</sup> Since the Arg258 has already rotated to hydrogen-bond with Tyr296 early in the simulation with both ions, we cannot predict from this trajectory when the full Arg258 rotation from open to closed state occurs in pol  $\beta$ 's closing. However, the estimates of the closing free energy profile based on the coarse-graining approximation suggest that a slow, rate-limiting step is associated with the partial rotation of Arg258.<sup>59</sup>

For the simulation with no ions before the chemical reaction, the Phe272 ring flip is pronounced and also Arg258 rotates toward Asp192 to form a salt bridge. Distance evolutions (Arg258:NH1 to both Asp192:O $^\delta$  and Tyr296:OH) in Figure S2 indicate formation of the Arg258:NH1 and Asp192:O $^\delta$  salt bridge and breakage of the Arg258:NH2 and Tyr296:OH hydrogen bond, with the former event slower than the thumb opening. We also note that Tyr296 moves further away from Arg258 when no ions are present compared to the other systems, likely due to the breakage of the Arg258:NH2/Tyr296:OH hydrogen bond. This Tyr296 flexibility has also been observed in our prior simulation for the R258A mutant,<sup>53</sup> in which the

(59) Radhakrishnan, R.; Schlick, T. *Proc. Natl. Acad. Sci. U.S.A.* **2004**, *101*, 5970–5975.



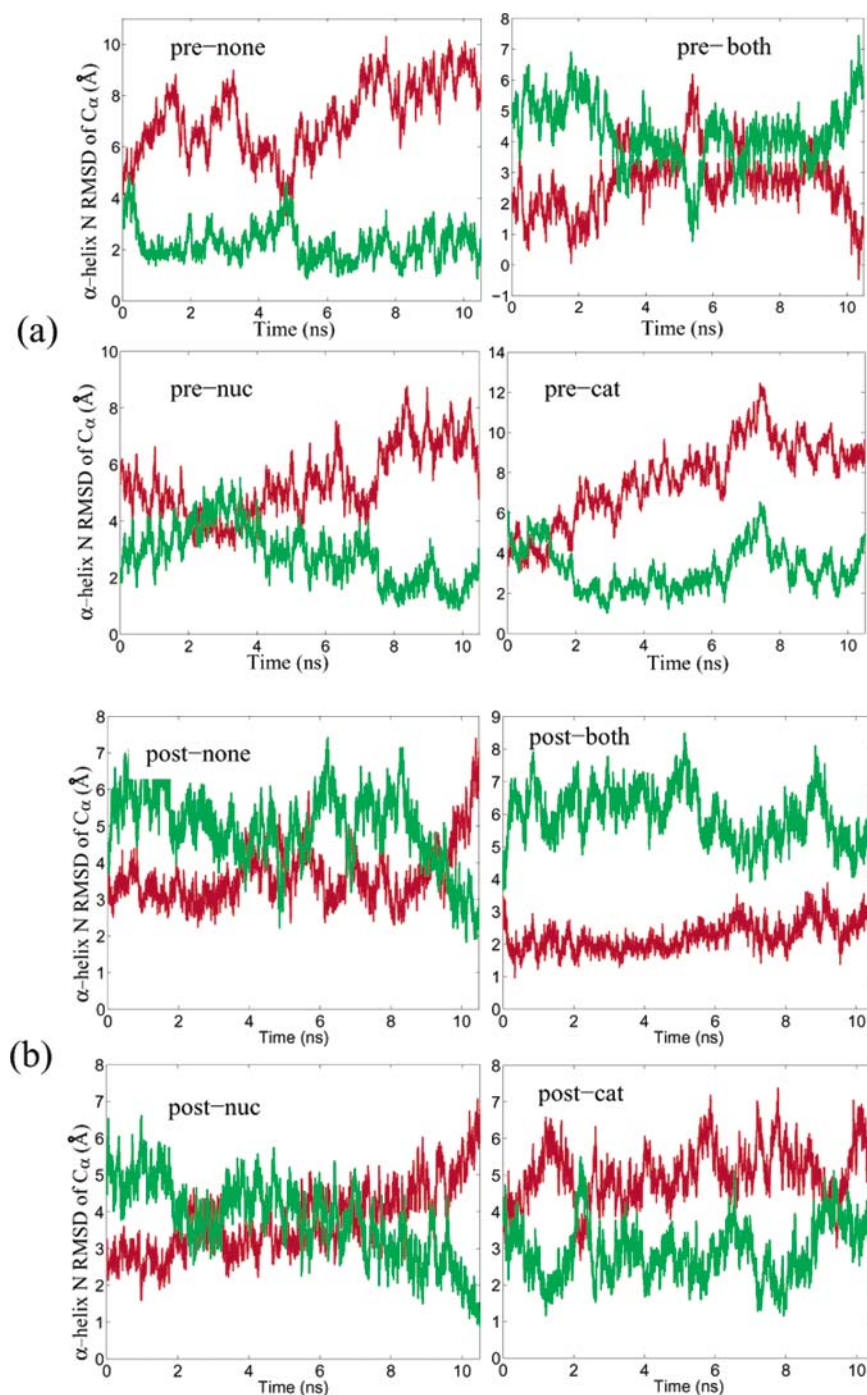


**Figure 3.** The evolution of RMSD for the  $\alpha$ -helix N  $C^{\alpha}$  atoms in the simulations (a) before and (b) after the chemical reaction of nucleotide incorporation relative to the crystal closed (red) and open (green) structures. Note that the rmsd values for pre-both simulation (top right in panel (a)) are modified since its  $\alpha$ -helix N moves significantly parallel to those in the crystal closed and open structures. See details for the processing method in the Supporting Information. Superimpositioning is performed according to the palm  $C^{\alpha}$  atoms.

Arg258/Tyr296 hydrogen bond also broke. When only one ion is present before the chemical reaction, Phe272 ring flips very early in the simulations (Figure 4), and the complete thumb opening follows. Arg258 remains midway between Tyr296 and Asp192 in the simulation with the nucleotide-binding  $Mg^{2+}$  only while the Arg258:NH/Tyr296:OH hydrogen bond is formed in the simulation with the catalytic  $Mg^{2+}$  only. Therefore, our dynamics simulations with one or no ions together suggest a sequence of events in pol  $\beta$ 's opening *before the chemical reaction*: (I) Phe272 ring flip; (II) thumb movement to an open state; and (III) Arg258 rotation toward Asp192 to form a

hydrogen bond. This agrees well with the sequence of events in pol  $\beta$ 's opening *after the chemical reaction* proposed by our prior simulations for the wild-type pol  $\beta$ /DNA complexes without both  $Mg^{2+}$  ions.<sup>48,49,53</sup> In particular, our previous accelerated sampling (high-temperature simulations and TMD simulations)<sup>48,49</sup> suggests that Arg258's side chain rotation could be slow enough to be kinetically significant.

Site-directed mutagenesis studies are consistent with our proposed role for Arg258. We observed that the alanine mutation for Arg258 facilitates the thumb closing in our prior simulation<sup>53</sup> and thus may explain the experimentally determined increased

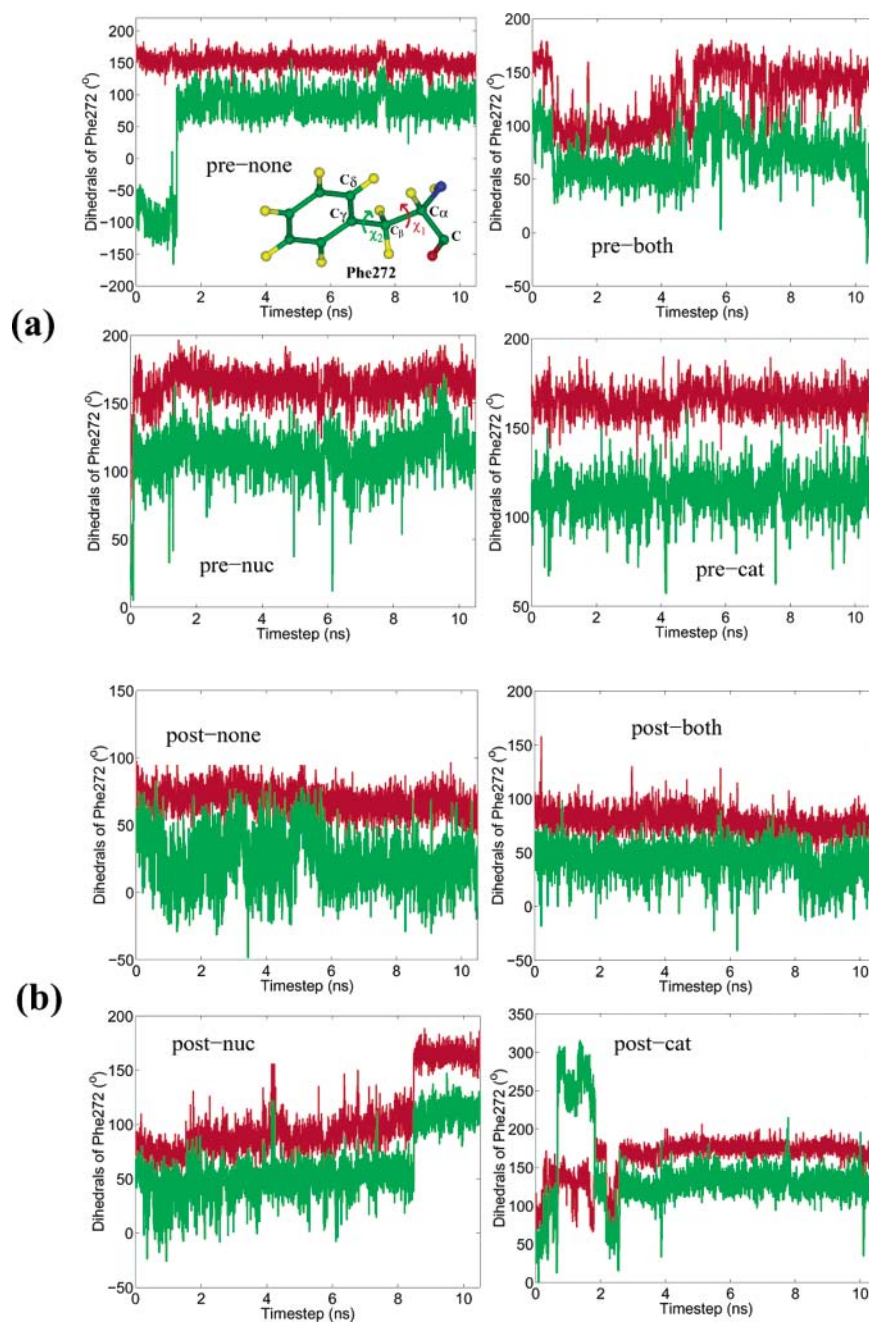


**Figure 4.** Time evolution of two dihedral angles associated with the Phe272 phenyl ring over the trajectories of both (a) before and (b) after nucleotide chemical incorporation. The two dihedral angles of Phe272 are defined by the following atomic sequence:  $\chi_1$  (red) for C–C $^\alpha$ –C $^\beta$ –C $^\gamma$  and  $\chi_2$  (green) for C $^\alpha$ –C $^\beta$ –C $^\gamma$ –C $^\delta$ .

rate of nucleotide insertion in this mutant with respect to the wild-type enzyme (ref 60; W. A. Beard, D. D. Shock, and S. H. Wilson, unpublished data). These results indicate that the chemical character of the residue at position 258 can influence the rate-determining step. Interestingly, Arg258 is not conserved among other X-family polymerases,<sup>53</sup> suggesting that Arg258 modulates nucleotide insertion for pol  $\beta$  in a manner that may influence its biological activity in base excision repair. A corresponding arginine residue exists at position 660 in the  $\alpha$ -helix O of the Taq DNA polymerase. Mutating this Arg660 was found to selectively reduce ddGTP incorporation, mainly

due to an additional hydrogen bond that Arg660 makes with ddGTP relative to the other three incoming nucleotides.<sup>12,13</sup> Thus, the combined results of our dynamics simulations,<sup>53</sup> transition path sampling studies,<sup>59</sup> and experimental kinetic measurements (W. A. Beard, D. D. Shock, and S. H. Wilson, unpublished data) for the R258A mutant suggest a “gate keeping” mechanism of Arg258 to the active site assembly (T. Schlick et al., unpublished).

In our postchemistry simulations with one ion, the Phe272 ring flip occurs prior to the pol  $\beta$  opening. For example, the Phe272 ring flip and thumb opening occur at about 8.4 ns and 9.6 ns, respectively, in the simulation with the nucleotide-binding Mg<sup>2+</sup> only, while they occur at about 0.25 ns and 1.2 ns, respectively, in the simulation with the catalytic Mg<sup>2+</sup> only

(60) Menge, K. L.; Hostomsky, Z.; Nodes, B. R.; Hudson, G. O.; Rahmati, S.; Moomaw, E. W.; Almasy, R. J.; Hostomska, Z. *Biochemistry* **1995**, *34*, 15934–15942.

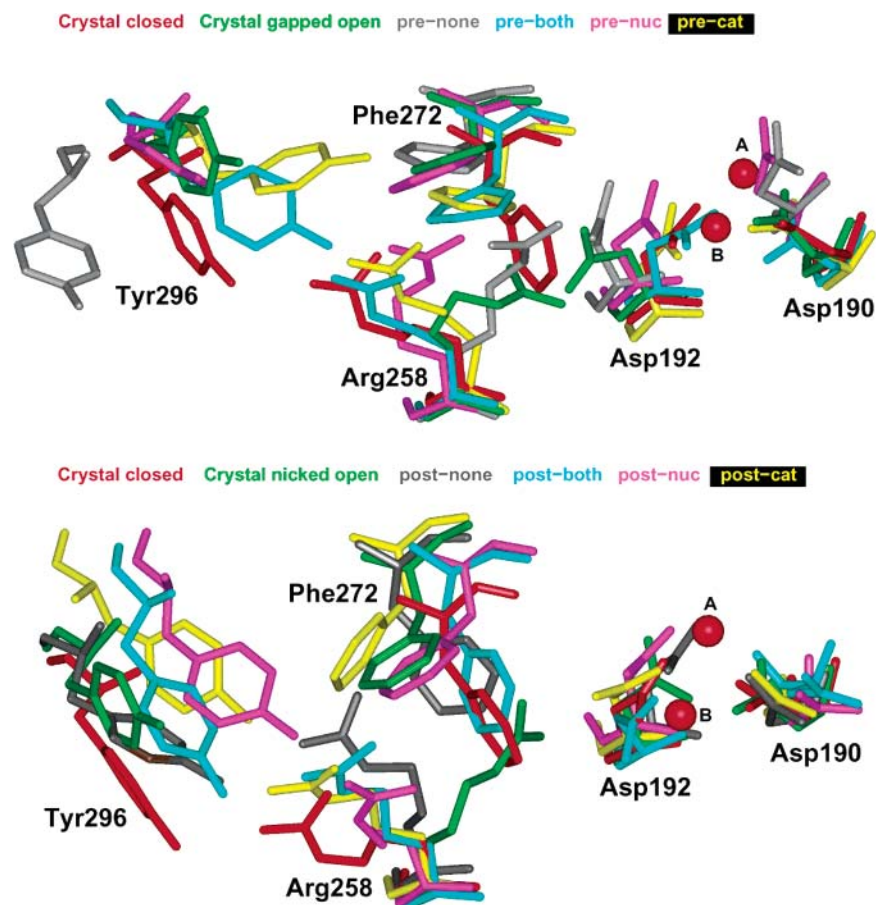


**Figure 5.** Conformational comparisons for several active-site protein residues in the simulated systems both before (upper) and after (lower) the chemical reaction and in the crystal closed (red) and open (green) structures. The colors gray, cyan, pink, and yellow indicate the simulated pol  $\beta$ /DNA complexes with no  $Mg^{2+}$ , both  $Mg^{2+}$ , the nucleotide-binding  $Mg^{2+}$ , or the catalytic  $Mg^{2+}$ , respectively. The open crystal reference is the binary gapped pol  $\beta$ /DNA complex for the simulated systems before the chemical reaction (upper), while the binary nicked pol  $\beta$ /DNA complex is the reference for the simulated systems after the chemical reaction (lower).

(Figures 3 and 4). Although the Phe272 ring flip is not observed in the postchemistry simulation with no ions here, it occurs in our prior simulations for the same pol  $\beta$ /DNA complex after the chemical reaction.<sup>48,49,53</sup> Arg258 does not rotate toward Asp192 in all the postchemistry simulations with one or no ions. Thus, the sequence of events in pol  $\beta$ 's opening proposed by the above prechemistry simulations also applies to the postchemistry simulations.

At the start of the simulation with both ions after the chemical reaction (post-both), the thumb is in a partial closed state, Asp192 coordinates both  $Mg^{2+}$  ions, and Arg258 rotates to form a hydrogen bond with Tyr296. The Phe272 is midway between Arg258 and Asp192 and does not flip at all through the entire post-both simulation, similar to that in the crystal closed structure. This trajectory suggests that the above proposed sequence of events in pol  $\beta$ 's closing *before the chemical reaction* also applies to the pol  $\beta$ 's closing *after the chemical reaction*.

In sum, the studies here help suggest a specific sequence of events during pol  $\beta$ 's closing and opening motions both before and after the chemical reaction of nucleotide incorporation that rely crucially on systematic ion rearrangements as well as enzyme side chain motions.

**3.3. Magnesium Coordination before and after the Chemical Reaction.** We observe that the nucleotide-binding and/or catalytic  $Mg^{2+}$  remain in the active site throughout all simula-

tions. Each  $Mg^{2+}$  coordinates six ligands including several water molecules to form a nearly perfect octahedral coordination sphere in all systems. Figure 6 presents the magnesium coordination patterns in the active site for all systems after a 10.5 ns simulation, and Table 1 lists the ligands coordinated to all magnesium ions. The ligands for each magnesium are stable throughout all simulations except those for the catalytic magnesium ion in the simulation with only that ion before the chemical reaction, in which the coordinated water molecule exchanges with waters in solution. Such exchange of first shell water molecules of magnesium ion on the nanosecond time scale simulation rather than microsecond time scale probably results from the inherent understabilized interactions of divalent ions in the force field.

In the simulation with both ions before the chemical reaction, the catalytic  $Mg^{2+}$  strongly coordinates Asp190, Asp192, Asp256, the  $\alpha$ -phosphate of dCTP, and a water molecule, similar to the catalytic  $Mg^{2+}$  coordination in the crystallographic closed ternary complex.<sup>16</sup> In addition, this catalytic  $Mg^{2+}$  weakly coordinates P10:O3' which is absent in the crystallographic closed structure. Moreover, the weak magnesium coordination with P10:O3' (e.g., 4.7 Å) suggests that the polymerase active-site geometry has not approached the perfect catalytic position ready for the chemical reaction of nucleotide incorporation to the primer 3'-terminus in the simulation with both ions, although it has moved somewhat toward a closed state; this, in part, may



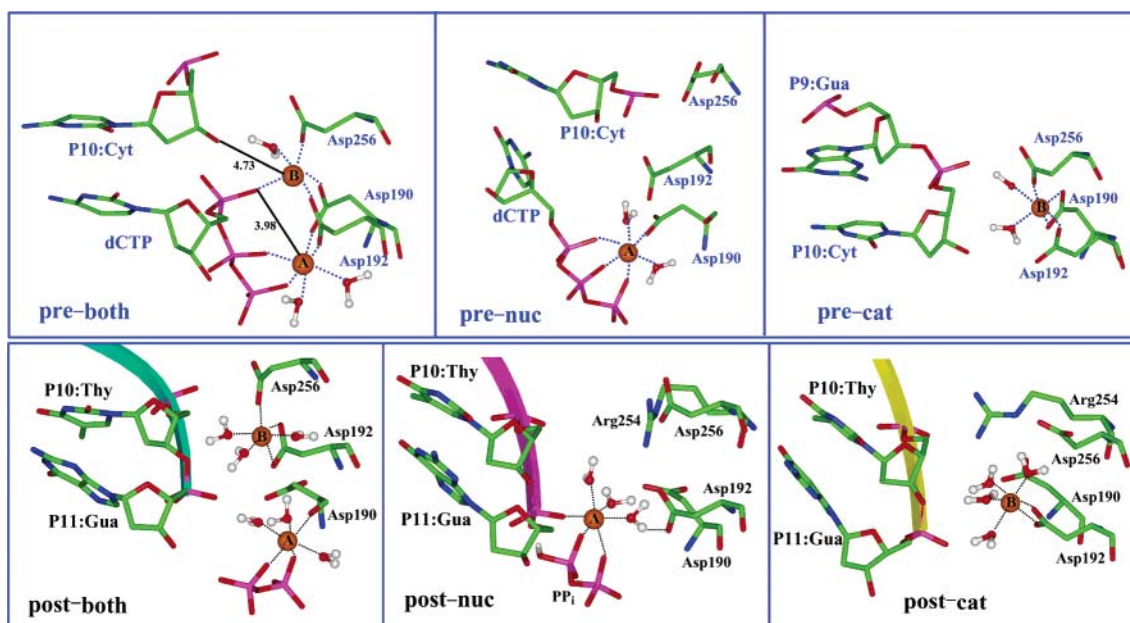


**Figure 6.** Coordination of the magnesium ions in the active site of the systems (upper) before and (lower) after the nucleotide chemical incorporation (with one or both Mg<sup>2+</sup> ions) after a 10.5 ns simulation. The ligands for each magnesium ion in the simulated systems are presented in Table 1, and the ion ligands in both crystal closed and open structures are also given for comparison.

**Table 1.** Magnesium Coordination in Simulated Systems and Crystal Closed Ternary Complex<sup>a</sup>

system	nucleotide-binding Mg <sup>2+</sup>	catalytic Mg <sup>2+</sup>
crystal closed	$\alpha, \beta, \gamma$ -phosphate O, Asp190:O <sup><math>\delta</math></sup> , Asp192:O <sup><math>\delta</math></sup> , H <sub>2</sub> O	$\alpha$ -phosphate O, P10:O3', Asp190:O <sup><math>\delta</math></sup> , Asp192:O <sup><math>\delta</math></sup> , Asp256:O <sup><math>\delta</math></sup> , H <sub>2</sub> O
pre-nuc	$\alpha, \beta, \gamma$ - <b>phosphate O, Asp190 O<sup><math>\delta</math></sup></b> , 2 H <sub>2</sub> O	X
pre-cat	X	<b>2 Asp190:O<sup><math>\delta</math></sup>, Asp192:O<sup><math>\delta</math></sup>, Asp256:O<sup><math>\delta</math></sup>, H<sub>2</sub>O</b>
pre-both	$\beta, \gamma$ - <b>phosphate O, Asp190:O<sup><math>\delta</math></sup>, Asp192:O<sup><math>\delta</math></sup></b> , 2 H <sub>2</sub> O	<b><math>\alpha</math>-phosphate O, H<sub>2</sub>O, Asp190:O<sup><math>\delta</math></sup>, Asp192:O<sup><math>\delta</math></sup>, Asp256:O<sup><math>\delta</math></sup>, P10:O3'</b>
pre-nuc	2 PP <sub>i</sub> :O, P11:O <sub>2</sub> P, 3 H <sub>2</sub> O	X
post-cat	X	Asp190:O, <b>Asp192:O<sup><math>\delta</math></sup>, 4 H<sub>2</sub>O</b>
post-both	2 PP <sub>i</sub> :O, Asp190:O, 3 H <sub>2</sub> O	<b>2 Asp192:O<sup><math>\delta</math></sup>, Asp256:O<sup><math>\delta</math></sup>, 3 H<sub>2</sub>O</b>

<sup>a</sup> Bold items correspond to the same interaction as in the crystal forms.

reflect force-field parameters and limited sampling as well, since the simulations cover a very small time compared to the likely long time scale of active site organization.

We find that coordinations for the same magnesium ion (nucleotide-binding or catalytic) are somewhat different among the simulated systems. For example, before the chemical reaction, the nucleotide-binding Mg<sup>2+</sup> coordinates the  $\alpha$ -phosphate oxygen in the presence of the nucleotide-binding ion only while it does not when both ions are there. After the chemical reaction, the catalytic Mg<sup>2+</sup> coordinates Asp256:O <sup>$\delta$</sup>  in the simulation with both ions, while it does not when only the catalytic Mg<sup>2+</sup> is present. Such different magnesium coordination patterns are possibly associated with different polymerase conformations (closed, open, partial closed, or partial open) and the attempt of ion(s) to achieve charge neutrality in a highly charged system. In addition, it shows that the lack of one Mg<sup>2+</sup> would affect the coordination pattern of the other Mg<sup>2+</sup>. Therefore, the coordination patterns of one or both magnesium ions as well as their synergetic effects on the active site geometry may affect the polymerase closing/opening trends.

**3.4. Na<sup>+</sup> or Mg<sup>2+</sup> Diffusion into the Active Site in Simulations after the Chemical Reaction.** Interestingly, we find that one Na<sup>+</sup> counterion from the solution moves to coordinate Asp190, Asp192, and/or Asp256 in the active site in the postchemistry simulation lacking both divalent ions (post-none). As shown in Figure 7a,b, this Na<sup>+</sup> diffuses from more

than 30 Å away from the active site through a pol β tunnel formed by thumb, palm, and fingers subdomains to first coordinate P10/Thy:O2P, and following a stable coordination with P10/Thy:O2P for ~2ns, this Na<sup>+</sup> moves to interact with Asp190, Asp192, and/or Asp256 during the remaining 2 ns simulation (movie available on website [monod.biomath.nyu.edu/index/gallery.html](http://monod.biomath.nyu.edu/index/gallery.html)). Figure 7c shows a snapshot of the coordination arrangement of this Na<sup>+</sup> with Asp190, Asp192, and three water molecules. The water molecules coordinated to this Na<sup>+</sup> are nonspecific and exchange with other solution water molecules during the simulation. When we superimpose the simulated final structure onto the crystal closed complex (or the simulated post-both system) according to the palm subdomain, we find that this Na<sup>+</sup> site is midway between the nucleotide-binding and catalytic Mg<sup>2+</sup> sites in the two closed systems. The Na<sup>+</sup> position, also different from that of the Mg<sup>2+</sup> in a crystal pol β/DNA complex with a CA mispair after the chemical reaction (Krahn, Beard, and Wilson, submitted), likely acts as a surrogate electrostatically, but not functionally and structurally, for the missing Mg<sup>2+</sup> ions.

To investigate whether the divalent ion might diffuse into the active site, we have also modeled a *closed* pol β/DNA complex after the chemical reaction of dCTP incorporation to primer, with the nucleotide-binding Mg<sup>2+</sup> as well as its associated PP<sub>i</sub> product in the active site, a Na<sup>+</sup> in the catalytic position, plus another Mg<sup>2+</sup> in solution is located about 20 Å

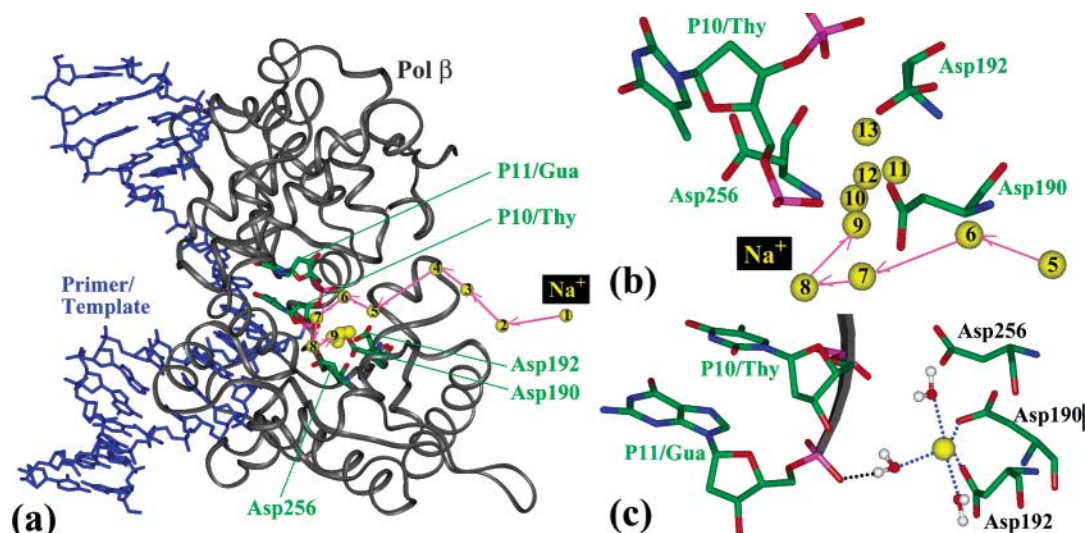


**Figure 7.** Dynamics pathway of a  $\text{Na}^+$  counterion diffusing into the active site (a and b) in the simulation with no  $\text{Mg}^{2+}$  ions after the chemical reaction and a snapshot of the sodium coordination with key residues Asp190, Asp192, and three water molecules (c). In panel a, the gray ribbon represents pol  $\beta$ , and the blue stick represents the primer/template duplex DNA. The numbered yellow balls in panel a and b sketch the  $\text{Na}^+$  diffusion pathway.

away from the active site. After the simulation over 7.6 ns, the solution  $\text{Mg}^{2+}$ , along with six coordinated water molecules, succeeds in moving into the active site through the tunnel formed by palm, thumb, and fingers subdomains within about 3 ns. As Figure 8a shows, the distance between the solution  $\text{Mg}^{2+}$  and the nucleotide-binding  $\text{Mg}^{2+}$  decreases from  $\sim 20.2$  Å at 3.2 ns to  $\sim 5.2$  Å at 6.3 ns. The coordination patterns of the nucleotide-binding  $\text{Mg}^{2+}$ , the solution  $\text{Mg}^{2+}$ , and the  $\text{Na}^+$  in the catalytic position are shown in Figure 8b,c. Since the radius of this six-water-ligated  $\text{Mg}^{2+}$  is relatively large (the average distance between this magnesium and the coordinating water oxygens is  $\sim 2$  Å), it is very difficult for this solution  $\text{Mg}^{2+}$  to move closer to coordinate Asp190, Asp192, and Asp256, even after the  $\text{Na}^+$  at the catalytic position is removed (data not shown). Indeed, exchanges between the liganded water molecules and the conserved protein residues (Asp190, Asp192, and Asp256) may require additional energy, similar to exchanging hydrogen bonds between incoming nucleotide/water molecules and the incoming nucleotide/template base as suggested by E. T. Kool.<sup>61,62</sup>

Interestingly, the  $\text{Mg}^{2+}$  diffusion pathway is similar to that we observe for the  $\text{Na}^+$  counterion: both pass through the pol  $\beta$  tunnel opposite the primer 3'-terminus. This suggests a readily available mechanism for ion diffusion that may be functionally relevant.

In addition, we note that when we replace the catalytic  $\text{Mg}^{2+}$  by  $\text{Na}^+$ , the sodium ion coordinates Asp190, Asp192, Asp256, P11 backbone oxygen, and one water molecule, very similar to the coordination of the catalytic magnesium in our simulated pre-both trajectory. This ties well with the experimental observation that a sodium instead of a magnesium in the polymerase catalytic position is present in a crystallographic ternary complex at a very high resolution of 1.65 Å (Krahn, Batra, Beard, and Wilson, unpublished data). This crystal structure involving a catalytic sodium confirms the mobility of a solution  $\text{Na}^+$  moving into the polymerase active site and the

crucial, tailored electrostatic environment available to the system at the active site.

### 3.5. dCTP Interacts with Ser180, Arg183, and Gly189 in the Simulated System with the Nucleotide-Binding Ion Only but with Asp192 and Asp256 when Both Ions Are Present before the Nucleotide Chemical Incorporation.

Figure 9 presents positions of the nascent base pair and protein residues that interact with the incoming dCTP before the chemical reaction; and the time evolution of certain protein/dCTP distances is shown in Figure S3. The dCTP moves somewhat away from the primer 3'-terminus by interacting with residues Arg149, Ser180, Arg183, Gly189, and Asp190 when only the nucleotide-binding ion is present, while the dCTP stays stable in the active site by interacting with residues Arg149, Asp190, Asp192, and Asp256 when both ions are present. The hydrogen bond between Tyr271:OH and dCTP:O2 is broken early in the former simulation but formed in the latter one. Moreover, residues Tyr271, Asp276, Asn279, and Arg283 move to interact with the template T6 in the simulation with both ions, while they move away from T6 in the other prechemistry simulations, as shown in Figure S4. These stabilizing networks of protein residues via hydrogen bonds and van der Waals contacts with the nascent base pair help interpret the subdomain motions, toward opening or closing, that we observed in the various systems and the roles of both divalent ions in triggering/stabilizing these rearrangements.

In addition, we find that the base of the template T6/dG deviates away from hydrogen-bonding with the incoming dCTP but partially stacks with the dCTP's base in the simulation with both ions (Figure 9b). Interestingly, we observe that, in the crystallographic intermediate of pol  $\beta$ /DNA with a CA mismatch (Krahn, Beard, and Wilson, submitted), the newly incorporated C in the primer strand is positioned below and partially stacks with the template A (Figure 9c). Such geometric distortions of the nascent base pair may inhibit the further full closing of the system with both ions before the chemical reaction.

### 3.6. Nascent Base Pair/Protein Interaction after the Chemical Reaction.

From the evolution of distances between two heavy atoms in each nascent GC/protein interaction pair in

(61) Kool, E. T. *Biopolymers* **1998**, *48*, 3–17.

(62) Kool, E. T.; Morales, J. C.; Guckian, K. M. *Angew. Chem., Int. Ed.* **2000**, *39*, 990–1009.

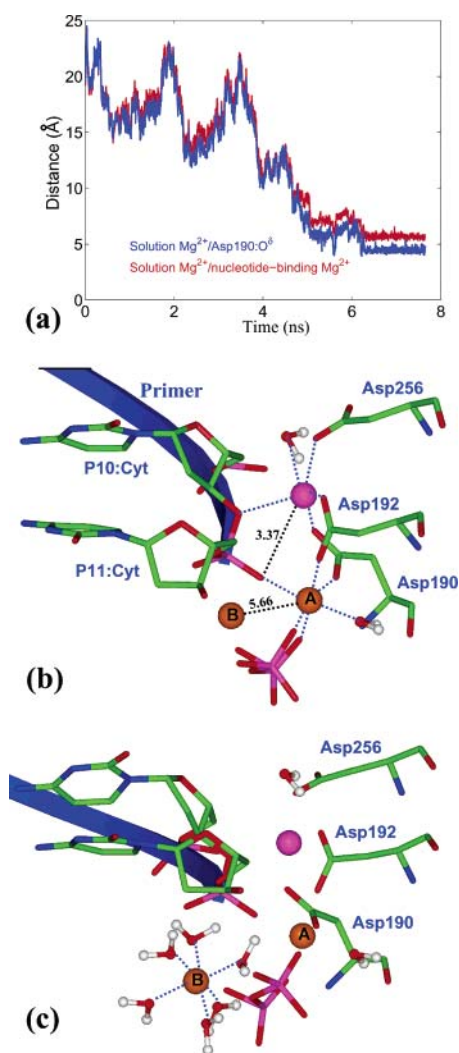


**Figure 8.** Time evolution of distances of the solution Mg<sup>2+</sup> with the nucleotide-binding Mg<sup>2+</sup> and Asp190:O<sup>δ-</sup> in the simulation of a closed pol β/DNA complex after the chemical reaction with the PP<sub>i</sub>/Mg<sup>2+</sup> association in the active site and a Na<sup>+</sup> in the catalytic position (a) and the corresponding ion coordinations patterns (b and c).

all four postchemistry simulations in Figure S3b, we note that the Tyr271:OH/P11:N3 hydrogen bond is weakly formed during all simulations except that it breaks early in the simulation with the catalytic ion only; this possibly results from the flexibility of P11:Gua. Asp276 makes van der Waals contact with P11/Gua at the start of all simulations, but this interaction is only retained in the simulation with both ions. The Arg283:NH1 and P11/Gua:N2 distance is out of the normal hydrogen bond range in all trajectories, whereas the template T6/Cyt:O2 hydrogen bonds with Arg283:NH1 and Lys280:N<sup>ε</sup> in certain intervals of the simulation with both ions. The Glu295:O<sup>ε</sup> hydrogen bond with the newly incorporated P11/Gua:N2H is maintained throughout the simulation when either both ions or only the nucleotide-binding Mg<sup>2+</sup> is present but persists for part of the trajectories when no ions or only the catalytic ion is present.

In general, our simulations reveal that protein residues Tyr271, Asp276, Lys280, Arg283, and/or Glu295 directly interact with the nascent GC base pairs in pol β's open and/or closed states after the nucleotide chemical incorporation, and this agrees with the above prechemistry simulations and our prior simulations for the pol β/DNA complexes with correct or

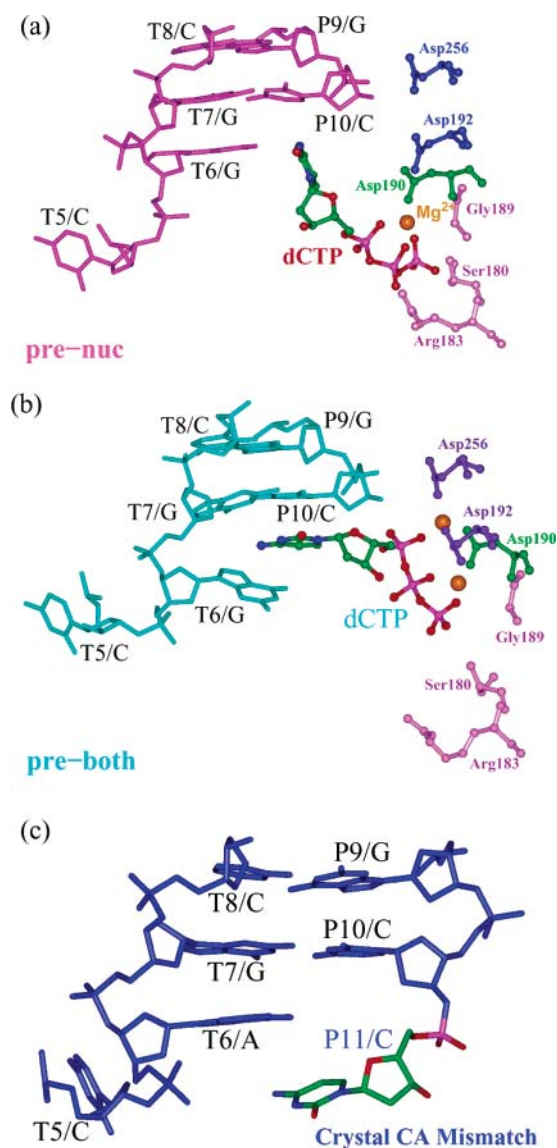


**Figure 9.** Conformations of the nascent base pair and several protein residues interacting with the incoming dCTP in the simulated systems (a) with the nucleotide-binding Mg<sup>2+</sup> only and (b) with both Mg<sup>2+</sup> and (c) in the crystallographic intermediate pol β/DNA complex with a CA mismatch after the nucleotide chemical incorporation.

incorrect base pairs.<sup>48,49</sup> The fact that we do not observe Glu295's interaction with the incoming nucleotide in the simulations before the chemical reaction is likely due to the distortion and/or movement of the nascent base pair in these systems. Kinetic analyses have also indicated that replacement of protein residues Tyr271,<sup>63,64</sup> Asp276,<sup>27</sup> Asn279,<sup>63,64</sup> Lys280,<sup>65,66</sup> and Arg283<sup>25,38,64,67,68</sup> can affect the catalytic efficiency and pol β fidelity in DNA synthesis. Therefore, our observation of the

- (63) Kraynov, V. S.; Werneburg, B. G.; Zhong, X.; Lee, H.; Ahn, J.; Tsai, M.-D. *Biochem. J.* **1997**, *323*, 103–111.  
 (64) Beard, W. A.; Osheroﬀ, W. P.; Prasad, R.; Sawaya, M. R.; Jaju, M.; Wood, T. G.; Kraut, J.; Kunkel, T. A.; Wilson, S. H. *J. Biol. Chem.* **1996**, *271*, 12141–12144.  
 (65) Beard, W. A.; Shock, D. D.; Yang, X.-P.; DeLauder, S. F.; Wilson, S. H. *J. Biol. Chem.* **2002**, *277*, 8235–8242.  
 (66) Kraynov, V. S.; Showalter, A. K.; Liu, J.; Zhong, X.; Tsai, M.-D. *Biochemistry* **2000**, *39*, 16008–16015.  
 (67) Osheroﬀ, W. P.; Beard, W. A.; Yin, S.; Wilson, S. H.; Kunkel, T. A. *J. Biol. Chem.* **2000**, *275*, 28033–28038.  
 (68) Osheroﬀ, W. P.; Beard, W. A.; Wilson, S. H.; Kunkel, T. A. *J. Biol. Chem.* **1999**, *274*, 20749–20752.



close contacts of these key protein residues with the nascent DNA base pair in the simulations both before and after the nucleotide chemical incorporation is consistent with their important roles in maintaining the faithful DNA synthesis.<sup>69</sup>

#### 4. Discussion

Our dissection of the effects of the nucleotide-binding and catalytic  $Mg^{2+}$  on pol  $\beta$ 's conformational transitions between closed and open states both before and after the nucleotide chemical incorporation helps delineate the various roles of these divalent ions on polymerase mechanisms and, in particular, associate them with key slow steps that direct nucleotide insertion apart from the chemical reaction itself.

**Closing of Thumb Subdomain Is Induced by Binding of Both  $Mg^{2+}$  Ions, and Opening Is Triggered by Release of the Catalytic  $Mg^{2+}$ .** Our finding that the dNTP/metal complex alone cannot induce polymerase closing before the chemical reaction and that both  $Mg^{2+}$  ions are required to prepare the active site for chemistry agrees with available experimental structures: open and closed crystallographic, ternary complexes of KlenTaq1 with both primer/template DNA and an incoming ddCTP<sup>11</sup> are found as open following dNTP/metal complex but closed with both  $Mg^{2+}$  ions in the active site. Our simulations provide atomic explanations to this requirement: the dCTP's triphosphate oxygens make van der Waals interactions with Ser180, Arg183, Gly189, and Asp190 when the catalytic ion is absent, instead of Asp190, Asp192, and Asp256. The former triplet likely pulls the dCTP away from the primer 3'-terminus, thereby facilitating pol  $\beta$  opening. The latter triplet of aspartates helps stabilize the incoming dCTP through interactions with both dCTP and the two functional  $Mg^{2+}$  ions.

Correspondingly, we deduce from our polymerase opening after the nucleotide chemical incorporation that the release of either the nucleotide-binding  $PP_i/Mg^{2+}$  or the catalytic  $Mg^{2+}$  helps trigger the opening. Again, experimental data corroborate these suggestions. From the observation of pyrophosphate-exchange experiments for DNA polymerase I (Klenow fragment)<sup>21</sup> that the second conformational transition (opening) occurs after the chemical bond formation but prior to the release of  $PP_i$ , it may be inferred that the catalytic metal ion leaves the active site before the  $PP_i$ /metal complex; otherwise, both metal ions in the active site could lock the polymerase in a closed state.

Therefore, we suggest that polymerase closing before the chemical reaction is induced by binding of both the dNTP/metal complex and the catalytic metal ion, while the polymerase opening after the chemical reaction is triggered by release of the catalytic metal ion, prior to release of the product  $PP_i$ /metal complex. Our proposed sequence of events in the pol  $\beta$  reaction pathway for nucleotide insertion differs from that proposed in ref 70 based on crystallographic closed structures with heavier ions (pol  $\beta$ -DNA-Cr(III)•dTMPCCP before the chemical reaction and pol  $\beta$ -DNA-Cr(III)•PCP after the chemical reaction) that closing is induced by the dNTP/metal complex prior to binding of the catalytic metal ion, while opening is induced by release of the  $PP_i$ /metal complex, possibly due to differences resulting from the use of  $Cr^{3+}$  rather than  $Mg^{2+}$ .<sup>70</sup> Our results further

suggest that protein residues Asp190, Asp192, and Asp256 play important roles in stabilizing the incoming nucleotide via van der Waals contacts with the nucleotide and liganding to the two functional  $Mg^{2+}$  ions.

**Possible Ion Heterogeneity/Fluidity at and near Active Site.** From our observations that a  $Na^+$  counterion diffuses rapidly from 30 Å away into the polymerase active site (within ~1 ns) after the chemical reaction, when no divalent ions are present, through a tunnel formed by thumb, palm, and fingers subdomains to coordinate Asp190, Asp192, and/or Asp256, we propose that electrostatic, though not functional, surrogates are possible. This ionic flexibility gains support from our prior simulations of pol  $\beta$ /DNA complexes with matched and mismatched DNA nascent base pairs<sup>48,49</sup> and from a very high-resolution (at 1.65 Å) crystallographic ternary complex of pol  $\beta$ /DNA/dCTP with a  $Na^+$  rather than a  $Mg^{2+}$  in the catalytic position (Krahn, Batra, Beard, and Wilson, unpublished data). Thus, the highly negative polymerase active site with conserved aspartates invites positive counterions and may tolerate some ion flexibility.

Together with our nanosecond-range observation of a magnesium ion diffusion from 20 Å away into the polymerase active site in a closed pol  $\beta$ /DNA complex after the nucleotide chemical incorporation in the presence of the nucleotide-binding  $Mg^{2+}$  and a  $Na^+$  in the active site, we suggest that binding of the catalytic metal ion is not a rate-limiting step in the polymerase reaction pathway. However, ion fluidity suggests that either  $Mg^{2+}$  ion may trigger the closing before the chemical reaction, depending on the situation at the active site. Namely, the catalytic  $Mg^{2+}$  can move into or out of the polymerase active site prior to binding of the dNTP/metal complex; once there, the dNTP/metal binding would induce the polymerase closing. If, on the other hand, binding of the dNTP/metal occurs prior to binding of the catalytic metal ion, the catalytic metal ion's motion into the active site would induce the closing. Thus, both metal ions must be present in the polymerase active site to trigger the closing subdomain conformational change.

**Possible Polymerase Reaction Sequence.** Both conformational events associated with transitions between closed and open states<sup>48,59,71,72</sup> and the nucleotide chemical incorporation<sup>73–75</sup> steps have been proposed as a rate-limiting step in polymerase reaction pathways. The collective picture that is now emerging, from kinetic data,<sup>27,40</sup> crystallographic structures,<sup>11,70</sup> dynamics simulations,<sup>48,49,53</sup> and transition path sampling studies,<sup>59</sup> is that slow conformational steps as well the chemical step contribute to the monitoring of polymerase fidelity. Even if the chemistry step is rate-limiting overall in the pathway, there exist subtle, slow side chain rearrangements in the pol  $\beta$ /DNA active site that allow the subdomain motion to occur<sup>48</sup> and that direct the system in a systematic way (via well-defined transition states)<sup>59</sup> to the reaction-competent closed state. Thus, conformational arrangements, involving Arg258, Asp192, Tyr271, and Phe272,<sup>59</sup> add checks and balances into the functional mechanisms by making the active site sensitive to changes; an incorrect nucleotide would likely disrupt this sequence of events (data in

(69) Kunkel, T. A.; Wilson, S. H. *Nat. Struct. Biol.* **1998**, *5*, 95–99.

(70) Arndt, J. W.; Gong, W.; Zhong, X.; Showalter, A. K.; Liu, J.; Dunlap, C. A.; Lin, Z.; Paxson, C.; Tsai, M.-D.; Chan, M. K. *Biochemistry* **2001**, *40*, 5368–5375.

(71) Johnson, K. A. *Annu. Rev. Biochem.* **1993**, *62*, 685–713.

(72) Bryant, F. R.; Johnson, K. A.; Benkovic, S. J. *Biochemistry* **1983**, *22*, 3537–3546.

(73) Showalter, A. K.; Tsai, M.-D. *Biochemistry* **2002**, *41*, 10571–10576.

(74) Herschlag, D.; Piccirilli, J. A.; Cech, T. R. *Biochemistry* **1991**, *30*, 4844–4854.

(75) Knowles, J. R. *Annu. Rev. Biochem.* **1980**, *49*, 877–919.

preparation). Supported by prior findings on the close relation between the metal ions and these subtle side chain motions,<sup>48,59</sup> we infer that the slow rearrangement of the catalytic Mg<sup>2+</sup> also plays an important role in attaining the correct state before the chemical reaction.

Taken together, we suggest the following sequence in pol  $\beta$ 's reaction pathway for correct nucleotide insertion: (1) binding of the dNTP/Mg<sup>2+</sup> association to the pol  $\beta$ /DNA in an open state; (2) binding of the catalytic Mg<sup>2+</sup> to the active site; (3) relatively fast conformational transition from an open to a closed state involving subtle residue motions; (4) slow, and possibly rate-limiting, assembly of the key amino acid residues, template bases, Mg<sup>2+</sup> ions, and the primer 3'-OH; (5) slow and possibly rate-limiting chemical step of the nucleotidyl transfer reaction; (6) release of the catalytic Mg<sup>2+</sup>; (7) relatively fast conformational transition from the closed to open complex state again involving subtle residue motions; (8) release of the product PP<sub>*i*</sub>/Mg<sup>2+</sup> unit. Steps 1 and 2 may be interchangeable depending on which Mg<sup>2+</sup> first binds to the polymerase/DNA active site.

This proposed sequence extends the current view by suggesting that the geometric adjustment of the catalytic groups may be a separate step in the polymerase reaction pathway. How

this sequence might change in the case of DNA mismatches at the primer terminus is currently under study. Already, data<sup>59</sup> suggest that a mismatch alters significantly the interactions involving the divalent ions, disfavoring the chemical reaction.

**Acknowledgment.** The work was supported by NSF Grant ASC-9318159 and NIH Grant R01 GM55164 to T.S.. Computations were supported by National Computational Science Alliance under MCA99S021N and utilized the NCSA SGI Origin2000. We thank Ravi Radhakrishnan and Suse Broyde for valuable discussions. Acknowledgment is made to the donors of the American Chemical Society Petroleum Research Fund for support (or partial support) of this research.

**Supporting Information Available:** The definition of rmsd and modified rmsd values. Figures for time evolution of interactive energies between  $\alpha$ -helix N and the nascent base pair in all simulations, distances of Arg258 with Asp192 and Tyr296 in prechemistry simulations, protein residues with nascent base pair in all simulations. This material is available free of charge via the Internet at <http://pubs.acs.org>.

JA049412O